Design and Analysis of a MOEMS Accelerometer Using All-dielectric Meta-materials Based on Fano Resonance

Mohammad Reza Karimipour[1,4], Azadeh Sadat Naeimi[2,4,*], Nader Javadifar[1,4], Mohammad Bagher Nasrollahnejad[3]

Abstract– This paper introduces a novel micro-opto-electro-mechanical-systems accelerometer that leverages a tunable all-dielectric meta-material. The device operates by modulating the wavelength of incident light-wave. The utilized metamaterial takes advantage of highly tunable ultra-sharp Fano resonance peaks to create a high-performance accelerometer, offering enhanced sensitivity and resolution. Simulation results indicate the functional attributes of the proposed sensor: a mechanical sensitivity of 0.13 nm/g, a linear measurement range spanning ±38.4g, and an overall sensitivity of 1.17 nm/g. These characteristics render the device applicable across a broad spectrum of uses, from consumer electronics to inertial navigation.

Keywords: Accelerometer, MOEMS, Meta-material, Fano resonance, wavelength modulation

1-Introduction

In recent years, there's been a surge in commercializing high-performance MEMS inertial sensors for diverse applications. Among these, MEMS accelerometers stand out as one of the most appealing types in fields like navigation, aerospace, automotive, and more.

Every MEMS accelerometer has a crucial mechanical part including a rigid frame that supports a seismic mass with a set of springs. When the system experiences external acceleration, this mass moves along a certain axis in relation to the frame. So, it's important to measure how much this mass moves to figure out the applied external acceleration. Different methods have been used to track this movement, like capacitive [1, 2], piezo-resistive [3, 4], piezo-electric[5, 6] and optical [7-10]. Among these, capacitive sensing technique is the most popular one due to its ease of fabrication and relatively high performance, but it's not perfect. Sometimes, especially for specific tasks needing really high accuracy, capacitive method might not be the best choice[8].

The optical sensing approach is seen as a better option because it offers higher resolution, accuracy, and sensitivity compared to other sensing methods. Additionally, optical approaches provide natural immunity against Electro Magnetic Interference (EMI), making them suitable for EMI-contaminated and harsh environments[11]. However, the processes for making and packaging these sensors are quite expensive and complex[7].

An optical MEMS accelerometer operates by using the modulation of light-wave properties due to applied acceleration. There have been recent developments in optical accelerometers employing various methods like intensity modulation[12], wavelength modulation [7, 13], photo elastic effect[14, 15], and phase modulation [16]. Each method has its own pros and cons. For example, intensity modulation methods are simpler to implement in terms of the optical detection system and the required light source. However, they're highly sensitive to fluctuations in the light source, which can impact the device's performance. Wavelength modulation technique could be a good alternative to overcome this problem. While the wavelength modulation method can address this issue, it requires a high-quality light source, and a complex read-out system is needed to detect the wavelength shifts caused by acceleration. This complexity can increase the cost and fabrication complexity of the accelerometer.

This paper introduces a new Micro-Opto-Electro-Mechanical System (MOEMS) accelerometer, which relies on a mechanically adjustable all-dielectric meta-material based on Fano resonance phenomena. The meta-material proposed here comprises pairs of bar antennas with bent arms situated on top of a silica substrate. This silica layer serves as both the MEMS part and the bottom layer of the meta-material. The device offers high sensitivity, a broad measurement range, and excellent resolution, making it suitable for various applications, from automotive use to inertial navigation.

The rest of this paper is structured as follows: Section 2 explains the working principle of the meta-material and the proposed accelerometer. Section 3 is dedicated to design and analysis of the mechanical and optical parts using an analytical method and a frequency domain solver by CST

1 Department of Electrical Engineering, Aliabad Katoul Branch, Islamic Azad University, Aliabad Katoul, Iran.
2* Corresponding Author: Department of Physics, Aliabad Katoul Branch, Islamic Azad University, Aliabad Katoul, Iran. Email: Naeimi.a.s@gmail.com.
3 Department of Electrical Engineering, Gorgan Branch, Islamic Azad University, Gorgan, Iran.
4 Energy Research Center, Aliabad Katoul Branch, Islamic Azad University, Aliabad Katoul, Iran.

Received: 2024.05.27; Accepted: 2024.07.11

MWS software. Section 4 provides a comparative study between the proposed device and several similar works. Lastly, Section 5 ends up with a summary and concluding remarks.

2- Operating Principle

2.1. Operating principle of the proposed tunable meta-material reflector

As noted earlier, the core part of the proposed accelerometer is an all-dielectric meta-material with asymmetrical geometry. Generally, optical meta-materials consist of artificially engineered structures exhibiting unprecedented optical properties beyond natural materials. Our proposed meta-material acts as a reflector with discriminated optical resonance modes of frequencies that are depend on the geometrical features and utilized materials of the unit cell of the meta-material. The utilized meta-material is similar to the one we presented earlier in our previous work(see Figure 1) [17].

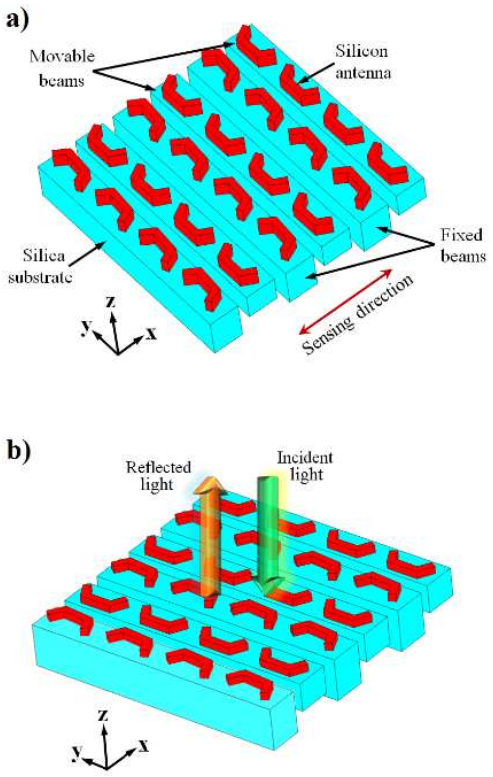

Figure 1: Operating principle of the meta-material. (a) 3D schematic and, (b) the operating principle of the proposed meta-material [17].

Our goal is to convert the proposed meta-material in to a tunable reflector, in order to sense mechanical displacements of the proof mass of the accelerometer. As shown in Figure 1(a), Transverse Magnetic (TM) polarized light is focused on the meta-material surface via an optical fiber. The incident light interacts with the meta-surface and is then reflected back to the output optical fiber which guides the reflected wave towards an optical photo detector. Initially, there could be a few wide-band resonance peaks, called dipole resonance modes, in the reflection spectrum of the meta-material. Central wavelength and amplitude of these modes are a criterion of the shape and consisting materials of a unit cell. According to the discussion provided in our previous work [17], In order to improve the device performance, one can introduce a geometrical symmetry into the structure of the unit cell resulting in the appearance of ultra-sharp Fano resonance modes in the reflection spectrum. As depicted in Fig. 2, this geometrical asymmetry can be introduced into the structure of the meta-material by changing the geometrical characteristics of one of the double antennas while the other one remains unchanged.By introducing this asymmetry into the

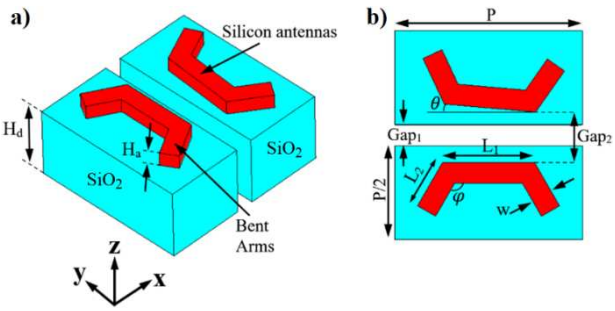

Fig. 2: Schematic of the unit cell of the proposed all-dielectric metamaterial, a) 3d view, b) top view.

antennas in each unit cell, a few additional ultra-narrow-band asymmetric resonance modes will appear in the reflection spectrum as a result of the Fano resonance phenomena [18-21]. These Fano peaks stem from the interference between the dipole (bright) and the quadrupole (dark) modes of the metamaterial. The appearance of these narrow-band peaks provides significant improvements in the performance of the sensing system in terms of resolution and sensitivity [22].

The most critical aspects to consider when analyzing the reflection spectrum diagram of the proposed device are the position of the resonance wavelength and its quality factor. Fig. 3 displays the reflection and transmission spectra of the suggested micro device for both symmetric and asymmetric unit cell configurations. The geometric parameters and their initial values are detailed in Table 1. When the geometric parameters remain at their initial values (as listed in Table 1) and assuming a completely symmetrical unit cell (θ=0), the structure does not exhibit any resonance peak within the desired wavelength range (Fig. 3, blue and red lines). Introducing structural asymmetry by slightly rotating one antenna (θ = 5°) while keeping the adjacent antenna in its original position creates an asymmetric structure, reflected in the red curve of the graph shown in Fig. 3. This figure illustrates a resonance peak with high reflectivity, crucial for reducing power consumption and improving the signal-to-noise ratio. Additionally, the Fano resonance peak demonstrates a relatively high quality-factor, meeting high-resolution requirements. To elaborate, the interference

between the quadrupole and dipole modes results in anti-phase oscillations, leading to minimal radiative loss at the respective wavelength. Consequently, an extremely sharp Fano resonance peak is achieved[23].

Table 1: Geometrical characteristics of a unit cell of the proposed metamaterial.

Parameters	Symbol	Value
Length of the middle arm of antenna1	La1	220 nm
Length of the middle arm of antenna2	La2	220 nm
Length of the bent arm of antenaa1	Lb1	120 nm
Length of the bent arm of antenaa1	Lb2	120 nm
Width of antenna1	W1	50 nm
Width of antenna2	W2	50 nm
Length and width of the unit cell	P	460 nm
The thickness of the silicon antennas	Ha	100 nm
The thickness of the silica layer	Hd	200 nm
The lateral distance between the top antennas	Gap2	45 nm
The lateral distance between the adjacent silica bars	Gap1	20-120 nm
The bent angle of the bent arm of antenna1	$\alpha 1$	45°
The bent angle of the bent arm of antenna2	$\alpha 2$	45◦
Deviation angle of the antenna2	θ	5◦
Total footprint of the sensor core for a 200×200 array	A	46×46 µm

The spectral behavior of the proposed all-dielectric meta-material can also be characterized using the Fano model which is mathematically described by the following formula [23].

$$T_{Fano} = \left|\left(a + jb + \frac{c}{\omega - \omega_0 + \mathrm{j}\gamma}\right)\right|^2 \quad (1)$$

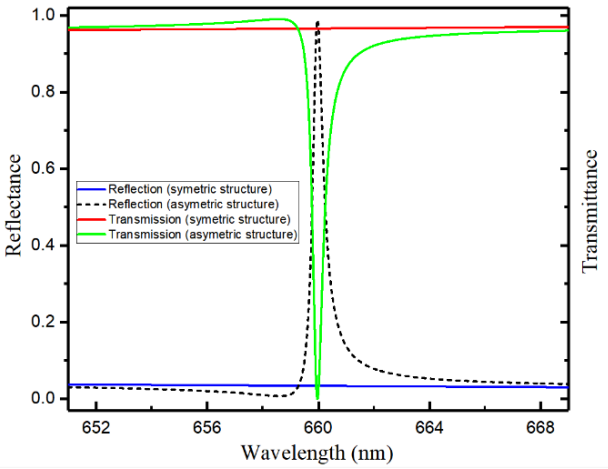

Fig. 3: Comparison between the reflection and transmission spectra of the symmetrical and asymmetrical structures [17].

where a and b are real numbers, c is a constant number, ω_0 is the Fano resonance frequency and γ is the total damping rate. As mentioned earlier, Fano resonance represents a distinct resonant phenomenon distinguished by its asymmetric line-shape [17].

2.2. Operating principle of the proposed optical MEMS accelerometer

The proposed MOEMS accelerometer is a wavelength modulation-based sensor. It means that the device detects the optical resonance mode shifts due to the displacements of the proof mass which is caused by the applied acceleration. A 3D schematic of the proposed accelerometer is shown in Figure 4. As can be seen from this figure, displacement sensing system of the proposed accelerometer is aall-dielectric meta-material reflector in which the movable beams of the meta-material are attached to an inner frameto realize a mechanically tunable reflector. Here, the proof mass consists of the movable beams and inner frame.

The proposed accelerometer functions in the following manner: Initially, the optical signal from the light source is transmitted to the surface of the meta-material via an optical fiber. The reflected light wave modes are then transferred to the output optical fiber and directed to a photo-detector, which links to a readout system. When an external acceleration is applied to the reference frame along the sensing axis in the positive direction (+x), the movable

beams of the meta-material move in the opposite direction along the same axis (-x). As depicted in Figure 6, this movement causes an increase in the gap size of the meta-material, potentially shifting the wavelength ofthe output Fano resonance mode towards larger wavelengths. Conversely, an applied acceleration in the negative direction along the sensing axis reduces the gap size, resulting in a shift of the wavelength of the output resonance mode towards smaller wavelengths. Ultimately, the readout system detects these wavelength shifts, allowing for the estimation of the amplitude and direction of the applied acceleration.

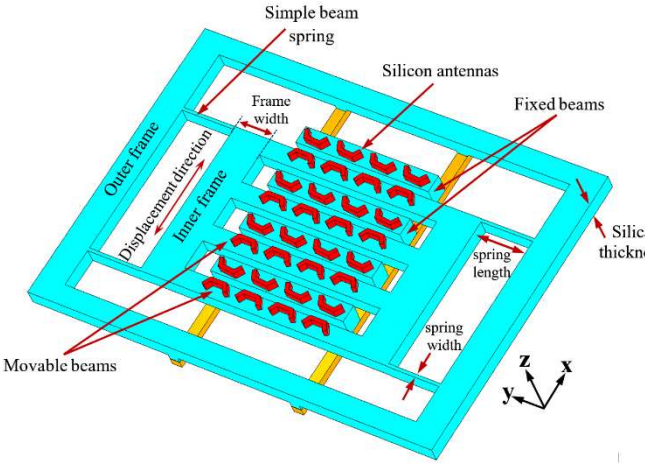

Figure 4: The structure of the proposed optical MEMS accelerometer.

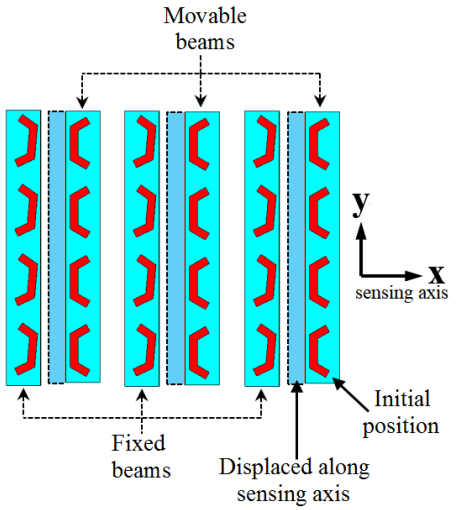

Fig. 5: Top view of the proposed structure, showing the initial position of the movable beams and their position after applying the displacement.

The proposed device can be fabricated on a Silicon-on-Insulator (SOI) wafer with top device layer thickness of 100nm, and SiO2 layer of 200nm thickness. The springs and proof mass can be fabricated on the SiO2 layerand the silicon antennas can be fabricated on the top device layer.

3-Simulations and materials

To explore the optical response of the proposed device, numerical analysis was conducted on the suggested metamaterial structure using CST Microwave Studio software (version 2019). The software was set up as follows: under MW & RF/OPTICAL | Periodic Structures | FSS, Metamaterial.

Unit cell boundary conditions were applied along the x- and y-axes, while open boundary conditions were set for the z-axis. The simulations utilized a frequency domain solver employing a tetrahedral meshing method. A plane wave with an electric component parallel to the Y-axis was directed perpendicularly onto the unit cell surface. Instead of examining the scattering parameters (S11 – S22), the built-in post-processing method was used to derive the reflection, transmission, and absorption spectra within the specified wavelength range.

4-Design and analysis of the mechanical and optical part of the accelerometer

4.1. Design and analysis of the mechanical part of the accelerometer

An accelerometer can be modeled mechanically as a two degree of freedom mass-spring-damper system as shown in Figure 6**Error! Reference source not found.**.

The dynamic behavior of such a system can be described by a second order differential equation [24].

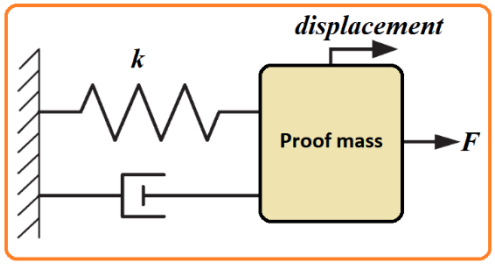

Figure 6: lamped model of mass-spring-damper system as a mechanical resonator.

$$F = m\ddot{d} + c\dot{d} + kd \qquad (2)$$

where F is the applied external force, m is the proof mass, c is the damping coefficient, k is the spring stiffness and d is the displacements of the proof mass.The performance of the accelerometer is significantly influenced by the physical and geometrical parameters of its mechanical part. The primary goal is to determine the spring stiffness (k) in both the sensing and perpendicular directions, calculated using the following formulas [25].

$$k_x = \frac{Ehw^3}{4L^3}, \quad (3)$$

$$k_y = \frac{Ewh^3}{4L^3}, \quad (4)$$

where k_x is the spring stiffness in the sensing direction, k_y is the spring stiffness in the perpendicular direction, E is the Young's modulus of silica, h is the thickness of the springs,w is the width of the springs, and L is the length of the springs. Here, Young's modulus of silica is chosen to be 66.3 GPa and the density of silica is 2170 kg/m^3.

According to Formula 2, one of the most important parameters of any accelerometer is the proof mass which affects the total behavior of the accelerometer. In this design, the overall mass of the proof mass is computed as the volume of the inner frame plus the volume of the movable beams, multiplied by the density of silica. The geometrical characteristics of the

Table 2: Geometrical characteristics of the mechanical part.

Parameters	Symbol	Value
Length of the springs	L	220 nm
Width of the springs	w	220 nm
Thickness of the springs (= silica layer thickness)	h	200 nm
Width of the inner frame	W	150 µm
Total footprint of the sensor core for a 200×200 array	A	~100×100µm

mechanical part, including the inner frame and the simple beam springs are addressed in Table 2.

Based on the desired application and chosen physical and geometrical parameters listed in Table 2, functional characteristics of the mechanical part of the proposed accelerometer can be derived using formulas 2, 3 and 4. The overall functionality of the proposed mechanical transducer can be determined by a feature called the mechanical sensitivity. This characteristic shows the way the applied acceleration is converted into mechanical displacements of the proof mass. For our proposed design, the mechanical sensitivity is calculated using the following formula[24]:

$$S_x = \frac{m}{k_x} \quad (5)$$

$$S_y = \frac{m}{k_y} \quad (6)$$

Where S_x is the mechanical sensitivity along sensing axis, S_y is the mechanical sensitivity along y-axis, m is the total proof mass, k_x and k_y are the spring stiffness in the sensing direction and perpendicular direction, respectively. It is desired to design the mechanical transducer to have a large sensitivity along sensing axis and zero sensitivity along perpendicular axis. Functional characteristics of the mechanical transducer used in this accelerometer are listed in Table 3.

Table 3: functional characteristics of the accelerometer. (gr: gram. g: m/s2, N: Newton)

Parameter	symbol	value
Proof mass (including inner frame and movable beams)	m	13.8 ngr
Spring constant along sensing axis(x)	k_x	0.106 N/m
Mechanical sensitivity along sensing axis (x)	S_x	1.3 nm/g
Spring constant along sensing axis(y)	k_y	2.65 N/m
Mechanical sensitivity along y axis	S_y	0.052 nm/g
Measurement range	R	± 38.4

In an accelerometer, a critical factor is its sensitivity to accelerations perpendicular to the sensing axis, ideally being zero. For our proposed accelerometer, the value of this parameter is small enough due to the negligible mechanical sensitivity in the sensing direction. This minimal sensitivity along the y axis is attributed to the use of simple beam springs, which provides significant stiffness in the y direction.

4.2. design and analysis of the optical displacement sensing system

As explained in section 2, movements of the meta-material's movable beamslead to alterations in the gap size of the antennas, subsequently resulting in a shift in the central wavelength of the output resonance mode.For more

clarifications, the initial position and displaced movable beam are depicted in Fig. 7.

In order to evaluate the effects of this displacements, a frequency domain analysis is performed using CST MWS software. In the simulations, the initial parameters listed in Table 1 and Table 2 are used and the gap width is varied from 0 to 150 nm using the parameter sweep. The effect of gap size changes on the output reflection spectrum of the proposed meta-material is shown in Fig. 8. As observed in the figure, the resonance mode's central wavelength undergoes a linear red shift (or blue shift) as the gap width is increased (or decreased). In essence, the proposed meta-material precisely converts the mechanical displacements of the movable beams into variations in the resonance wavelength. The performance of the optical sensing system used in the proposed device is determined as $S_o = \Delta\lambda/\Delta G$ which indicates the sensitivity of the sensing system to the displacements of the movable beams. Simulation results show that for our proposed displacement sensing system this

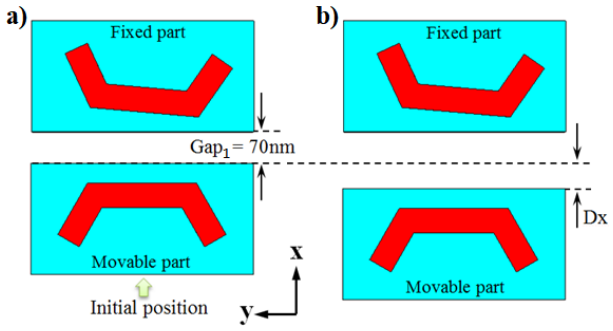

Fig. 7: Top view of the unit cell. a) initial position of the movable part; b) displacement of the movable beams along the sensing axis (Dx).

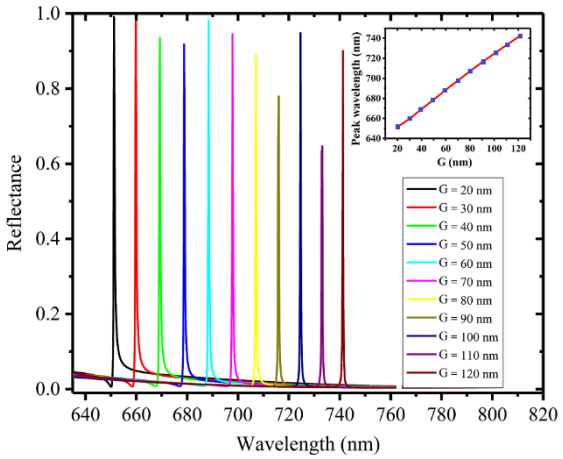

Fig. 8: The effect of gap size changes on the reflection spectrum of the suggested meta-material. the inset depicts the relationship between gap width (G) and the central wavelength of the Fano resonance.

sensitivity is about 0.9 nm/nm. To our knowledge, this level of optical sensitivity stands as the highest reported to date.

4.3. design and analysis of the proposed accelerometer

As already mentioned, in the proposed accelerometer, the central wavelength of the Fano resonance peak depends on the magnitude of the applied external acceleration. For the proposed accelerometer, the central wavelength shifts of the resonance mode versus changes of the meta-material's gap width and applied external acceleration is shown in Figure 9.According to the results shown in this figure, the response of this micro device is relatively linear (R2 = 0.9994) in the whole measurement range -38.4 g to 38.4 g). This linearity is due to the linear behavior of the proposed optical sensing system firstly and the mechanical resonator because of the employing springs in the suspension system secondly.

As previously stated, the central wavelength of the Fano resonance peak in the proposed accelerometer correlates with the magnitude of the applied external acceleration. Figure 9 illustrates the shifts in the resonance mode's central wavelength as a function of the variations in the meta-material's gap width and the applied external acceleration. The results depicted in this figure demonstrate a relatively linear response (R2 = 0.9994) across the entire measurement range from -38.4 g to 38.4 g. This linearity arises from the linear behavior of the proposed optical sensing system and,

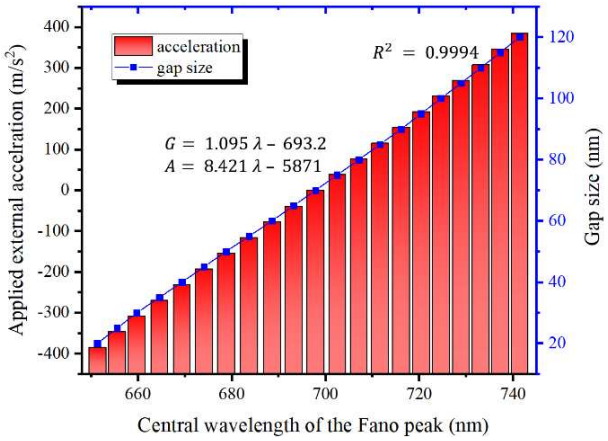

Figure 9: Central wavelength shifts (λ) of the reflected Fano resonance against external applied acceleration (A) as well as the gap size of the meta-material (G).

secondly, the mechanical resonator's characteristics due to the implementation of simple beam springs in the suspension system.

In order to determine the quality of the proposed accelerometer one can define a parameter named overall sensitivity ($S = \Delta\lambda/\Delta a$). The optical sensitivity for our proposed sensor is determined by the product of the optical sensitivity and the mechanical sensitivity along the sensing direction. Optical sensitivity of the proposed device is calculated to be around 1.17 nm/g.

5-Comparative study

In this section, we conduct a comparative analysis between our proposed accelerometer and some recent works [13, 14] within this domain. The main advantage of our proposed work over other recent contributions employing a wavelength modulation scheme is the ultra-high sensitivity of the optical sensing system, which is the highest reported sensitivity to date. This exceptional feature is attributed to the remarkable sensitivity of the Fano resonance peaks to external stimuli [20-23].

When considering the trade-off between sensitivity and the measurement range of the accelerometer, our device exhibits an overall sensitivity larger than that of other recent works, albeit with a smaller measurement range compared to its counterparts.

An additional critical parameter in wavelength modulation-based sensing systems is optical sensitivity, depicting wavelength shifts in response to proof mass displacements. In our proposed sensing system, this sensitivity is larger than all other works in this era.The summarized results of this comparative review are presented in Table 4.

Table 4:A comparative table between our proposed accelerometer and other recent works in this era**.**

parameter	This work	[7]	[8]	[9]	[10]
Footprint of the core part [µm]	100×100 µm	2.8×2.8 mm	400×400 µm	4×4 mm	-
Mechanical sensitivity [nm/g]	1.3	-	3.18	1009	130
Sensitivity of the optical sensing system [nm/nm]	0.9	-	0.368	0.032	0.026
Overall sensitivity of the accelerometer [nm/g]	1.17	1.63	1.17	32.9	3.4
Measurement range [g]	± 38.4 g	± 5.2 g	± 22 g	± 1 g	± 5 g

6-Conclusion

This paper introduces an integrated optical MEMS accelerometer that relies on an optical read-out approach. The device's optical sensing system is based on a wavelength modulation method, achieved using an LD light source, a photo-detector, and a mechanically tunable all-dielectric meta-material. Analytical and frequency domain simulations were conducted to study the mechanical structure and optical sensing system, respectively. The simulations provided the following functional characteristics for the proposed micro-device: a mechanical sensitivity of 0.13 nm/g, a linear measurement range of -38.4 g to 38.4 g, an optical sensitivity of 0.9 nm/g, an overall sensitivity of 1.17 nm/g, and negligible non-linearity across the total measurement range. These characteristics make it suitable for various applications, from consumer electronics to inertial navigation. The fabrication of the proposed MOEMS accelerometer using Deep Reactive Ion Etching is an ongoing effort, which could be the subject of a separate paper.

REFERENCES:

[1]I. Odira, J. Keraita, and J. Byiringiro, "Multimode TED-tuned beam mass damper for low-g capacitive MEMS accelerometers VRE reduction," Journal of Vibration and Control, p. 10775463231190442, 2023.

[2]W. Liu et al., "The High-Efficiency Design Method for Capacitive MEMS Accelerometer," Micromachines, vol. 14, no. 10, p. 1891, 2023.

[3]A. Khlifi et al., "Theoretical and numerical investigation of a new 3-axis SU-8 MEMS piezoresistive accelerometer," Microelectronics Journal, vol. 128, p. 105552, 2022.

[4]C. Jia et al., "Modeling and Characterization of a Novel In-Plane Dual-Axis MEMS Accelerometer Based on Self-Support Piezoresistive Beam," Journal of Microelectro mechanical Systems, vol. 31, no. 6, pp. 867-876, 2022.

[5]X. Gong, Y.-C. Kuo, G. Zhou, W.-J. Wu, and W.-H. Liao, "An aerosol deposition based MEMS piezoelectric accelerometer for low noise measurement," Microsystems & Nanoengineering, vol. 9, no. 1, p. 23, 2023.

[6] C. Yang, B. Hu, L. Lu, Z. Wang, W. Liu, and C. Sun, "A Miniaturized Piezoelectric MEMS Accelerometer with Polygon Topological Cantilever Structure," Micromachines, vol. 13, no. 10, p. 1608, 2022.

[7] L. Long, Z. Guo, and S. Zhong, "A MEMS accelerometer based on wavelength modulation using an integrated blazed grating," IEEE Sensors Journal, vol. 19, no. 3, pp. 877-884, 2018.

[8] A. Sheikhaleh, K. Abedi, and K. Jafari, "A proposal for an optical MEMS accelerometer relied on

wavelength modulation with one dimensional photonic crystal," Journal of Light wave Technology, vol. 34, no. 22, pp. 5244-5249, 2016.

[9] C. Trigona, B. Andò, and S. Baglio, "Design, fabrication, and characterization of BESOI-accelerometer exploiting photonic bandgap materials," IEEE Transactions on Instrumentation and Measurement, vol. 63, no. 3, pp. 702-710, 2014.

[10]M. Taghavi et al., "Closed-loop MOEMS accelerometer," Optics Express, vol. 30, no. 12, pp. 20159-20174, 2022.

[11] T. Guan, G. Keulemans, F. Ceyssens, and R. Puers, "MOEMS uniaxial accelerometer based on EpoClad/EpoCore photoresists with built-in fiber clamp," Sensors and Actuators A: Physical, vol. 193, pp. 95-102, 2013.

[12] A. Sheikhaleh, K. Abedi, K. Jafari, and R. Gholamzadeh, "Micro-optoelectromechanical systems accelerometer based on intensity modulation using a one-dimensional photonic crystal," Applied optics, vol. 55, no. 32, pp. 8993-8999, 2016.

[13] M. Ahmadian and K. Jafari, "A graphene-based wide-band MEMS accelerometer sensor dependent on wavelength modulation," IEEE sensors Journal, vol. 19, no. 15, pp. 6226-6232, 2019.

[14] W. Su, J. A. Gilbert, M. D. Morrissey, and Y. Song, "General-purpose photoelastic fiber optic accelerometer," Optical Engineering, vol. 36, no. 1, pp. 22-28, 1997.

[15] D. Tang, D. Zhao, Y. Wang, X. Zhang, Z. Liang, and F. Guo, "A MOEMS accelerometer based on photoelastic effect," Optik, vol. 122, no. 7, pp. 635-638, 2011.

[16] R. Wang, T. Li, S. Gong, and X. Qiao, "Multicore Fiber Based Phase-Modulation Interferometer for Demodulation of a Fiber Bragg Grating Accelerometer," Journal of Lightwave Technology, 2023.

[17] Karimipour, M.R., Naeimi, A.S., Javadifar, N., Nasrollahnejad, M.B., "A proposal for an ultra-sensitive nano-displacement sensing system based on all-dielectric metamaterials with tunable ultra-sharp Fano resonance peaks," Optical and Quantum Electronics, vol. 56, 2024.

[18] Q. Zhu et al., "Tunable graphene quadrupole dark mode based ultranarrow Fano resonance in asymmetric hybrid metamaterial," Optics Communications, vol. 510, p. 127927, 2022.

[19] Y. Liu et al., "Full control of fano spectral profile with gst-based metamaterial," ACS Photonics, vol. 9, no. 3, pp. 888-894, 2022.

[20] T. Xiang, T. Lei, J. Wu, J. Wang, and H. Yang, "Dual-Fano resonances based on all-dielectric toroidal metamaterial," Applied Physics Express, vol. 15, no. 3, p. 032002, 2022.

[21] H. Zhao et al., "All-dielectric metastructure based on multiple Fano resonances with high sensitivity," Optics Communications, vol. 530, p. 129193, 2023.

[22] A. Mashkour, A. Koochaki, A. Abdolahzadeh Ziabari, and A. Sadat Naeimi, "Demonstration of Tunable Fano Resonances in a Meta-material Absorber Composed of Asymmetric Double Bars with Bent Arms," Plasmonics, vol. 17, no. 4, pp. 1607-1618, 2022.

[23] M. Zhang, J. Fang, F. Zhang, J. Chen, and H. Yu, "Ultra-narrow band perfect absorbers based on Fano resonance in MIM metamaterials," Optics Communications, vol. 405, pp. 216-221, 2017.

[24] Y. Yang, I. I. Kravchenko, D. P. Briggs, and J. Valentine, "All-dielectric metasurface analogue of electromagnetically induced transparency," Nature communications, vol. 5, no. 1, p. 5753, 2014.

[25] G. K. Fedder, Simulation of microelectromechanical systems. University of California, Berkeley, 1994.